Pergamon

Available online at www.sciencedirect.com

SCIENCE DIRECT®

Cement and Concrete Research 34 (2004) 1025–1033

CEMENT AND CONCRETE RESEARCH

Computer simulation of fracture processes of concrete using mesolevel models of lattice structures

J.P.B. Leite[a,*], V. Slowik[b], H. Mihashi[a]

[a]Department of Architecture and Building Science, Tohoku University, Graduate School of Engineering, Aoba 06, Sendai 980-8579, Japan
[b]Hochschule für Technik, Wirtschaft und Kultur Leipzig (FH), D-04251 Leipzig, Germany

Received 22 July 2003; accepted 17 November 2003

Abstract

Mesolevel simulations were used to describe fracture processes in concrete. A new stochastic–heuristic algorithm was developed for generating the composite structure of concrete in 3-D space, producing specimens with comparably high aggregate content and realistic distribution. Aggregate particles were described as ellipsoids, allowing control in shape and size distributions. The continuum was discretised into lattices of linear elements, in structural analyses. For 2-D analyses, slices from the 3-D specimen were idealised as planar trusses/frames, while for the 3-D analyses the specimens were idealised as space structures. Fibre-reinforced concrete (FRC) was also modelled by introducing additional linear elements interconnecting distant nodes of the lattice. Compression, direct tension and wedge-splitting tests were simulated. Parametrical study was carried out to investigate the effect of different material properties and proportions in concrete admixtures. Simulation results are in agreement with experimental observations. Applicability and enhancements for such models are discussed and future research directions are proposed.

Keywords: Modelling; Microstructure; Interfacial transition zone; Fibre reinforcement; Softening

1. Introduction

Current phenomenological models, which assume concrete as a homogeneous material, have been of considerable relevance in structural design, as they may realistically predict the results of fracture processes in concrete. However, such models can neither estimate/describe the effects of the concrete composition on the macroscopic material behaviour nor contribute to material optimisations. For obtaining a deeper understanding of the physical processes determining the macroscopic material behaviour, models considering the heterogeneous nature of concrete are required.

Considerable differences of scale in the systems of concrete's internal structure do not allow the modelling of such systems as one. Hence, different models may be characterised by resolution ranges, which are usually determined by desired levels of detail and available computational power. As a general classification, mechanical models for concrete may be distinguished into three levels attempting to conform the scale to desired degrees of detailing of the material's structure. At a macroscopic level, the material is considered as homogeneous. Hence, models take no regard of the material composition. At the microscopic level, the structure of the cement paste is modelled, particularly the porous media. At the intermediary level, the mesoscopic level, the concrete is regarded as a two-phase material, either as small aggregates surrounded by the hardened cement paste or as coarse aggregate particles dispersed in a matrix of mortar. Mesolevel models have proved to be suitable for describing to a good extent the complex fracture behaviour of the concrete, as well as for investigating the influence of the concrete composition on the macroscopic properties [1,2]. However, the resolution range and applicability of mesolevel models may vary considerably from one to another. The increase of resolution range brings beneficial tractability but in general results in loss of physical detail.

Potential flaws of mechanical mesolevel models of concrete may be attributed to the limitations in producing

* Corresponding author. Tel.: +81-22-217-7893; fax: +81-22-217-7886.
E-mail address: jleite@timos.str.archi.tohoku.ac.jp (J.P.B. Leite).

0008-8846/$ – see front matter
doi:10.1016/j.cemconres.2003.11.011

realistic depictions of the highly heterogeneous internal structure of the concrete. The depicted concrete structure used in numerical models, referred to as numerical concrete, in most cases little resembles or does not resemble the real concrete material used in the correspondent empirical analysis. Thus the use of accurate stress analysis methods, or their results, may be highly questioned due to the inability of fictitious concrete structures to capture physical reality. While crude depictions have been capable of reproducing macro behavioural features, they are unlikely to describe the effects of different material properties of the concrete components, as well as effects of different admixtures, on the deformation and fracture behaviour. For mesolevel models to portray such effects, it requires creating an aggregate–matrix structure in a realistic way. Hence, the corresponding generation mechanism should fulfil the following requirements:

(i) The location of the aggregate particles should be free from correlations.
(ii) Shape and size of the particles should be randomly distributed within given limits.
(iii) The spatial aggregate distribution should be relatively uniform.
(iv) Given size distribution and content of the aggregates should be exactly matched.
(v) The maximum aggregate content should be as high as in the real concrete.

A new mechanism for generating a realistic aggregate–matrix structure is proposed. The mechanism generates 3-D concrete structures (Fig. 1), but it is equally suitable for both 2- and 3-D structural idealisations. 2-D concrete models are easily obtained by slicing the 3-D model (Fig. 2). Aggregate particles are assumed as ellipsoids, and by controlling the ratio between their three middle axes a variety of shapes may be obtained. The stochastic–heuristic scheme for allocating the aggregates, which has been embodied in the generation mechanism, allows for aggregate contents compared to the ones in real concrete and also for equivalent spatial distributions. In addition, the generation mechanism successfully meets all other requirements outlined above.

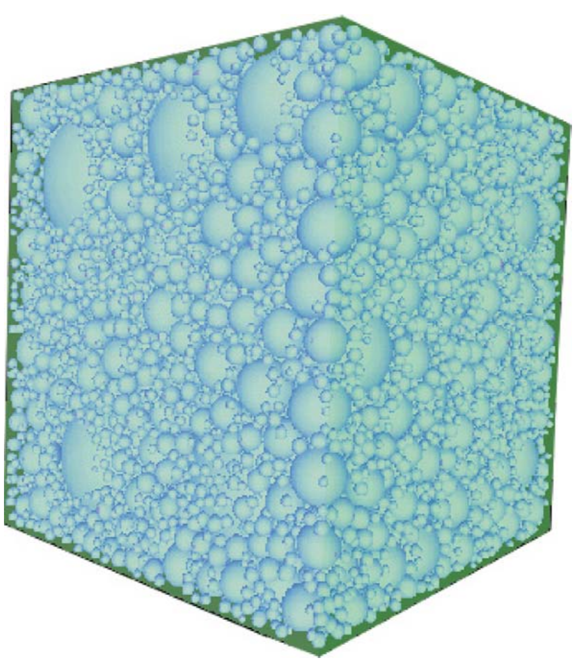

Fig. 1. Computer generated 3-D specimen with 60% aggregate content.

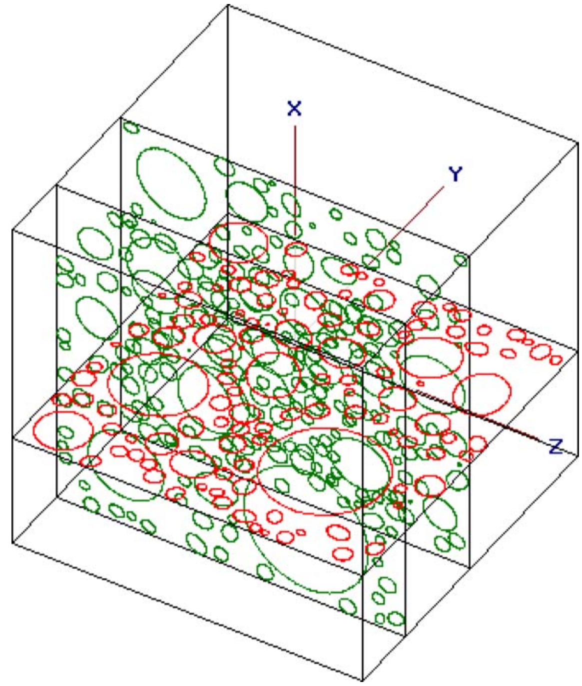

Fig. 2. Idealised slice cut-outs from a 3-D specimen for 2-D analyses.

2. Generation mechanism

The first three requirements, stated in the previous section, imply the usage of random number generators. In fact, the most trivial way of placing aggregate particles in the test volume or test area is to obtain the location purely randomly. When a particle is placed partially outside of the test volume or overlapping previously allocated particles, the trial location is dismissed and a new one is attempted. Although the simplicity of such a scheme is attractive, the efficiency is very poor. Practical computer random functions are in general linear congruential generators and therefore not free of sequential correlation on successive calls. In the particular case of 3-D spaces, the total number of planes in which triples of points could lie may be as low as the cube root of 32,768, or 32, and is unlikely to be larger than the cube root of 2^{32}, about 1600. This extremely pronounced discreteness of the planes prevents the exploration of small fractions of the volume. Therefore, such mechanisms are only capable of achieving comparably low aggregate contents, and the approach is extremely redundant and time consuming. In addition, the resulting mesolevel structure is a very coarse idealisation, which in general does not resemble the real concrete.

Vervuurt devised an improved mechanism [3] that simulates a process in which circular particles are dropped into a mould. The horizontal position for a particle is selected at random along the mould length. Thereafter the particle is moved downward until a specified minimum distance to particles previously placed is reached. To attain more dense structures, this procedure may be attempted several times for the same particle at different horizontal positions, selecting the deepest position from all attempts. The resulting structure may not be very uniform due to the formation of holes under the large aggregate particles. Another disadvantage of this more effective algorithm is that the aggregate content cannot be exactly predetermined. An alternative possibility of generating an aggregate–mortar structure is to discretise the test volume or the test area, similar to a finite element meshing. Then, the obtained volume or area sections are shrunk by a certain factor forming the particles [4]. In this way, aggregate contents up to 100% can be achieved. However, the obtained mesolevel structure is very different from those in real concrete samples.

In the proposed generation mechanism, the aggregate particles are idealised as ellipsoids. Depending on the material that they are intended to model, the ellipsoids may have to differ in size and roundness. An ellipsoid is uniquely defined in the 3-D space by specifying the lengths of its middle axes, the coordinates of its centre point and the directions of its axes (by Eulerian angles). The size can be limited by giving the grid lengths of two quadratic sieves, where the ellipsoid should be able to pass through the first but not through the second sieve. The specified aggregate volume for each sieve determines the size distribution. Adjusting the size of the last particles of each sieve attains the exact volumes for all sieves. Different shapes may be obtained according to the prescribed roundness. By roundness of an ellipsoid, it is intended to express how much the shape differs from that of a sphere. The roundness is prescribed by specifying a value or range for the ratio between the shortest and the longest middle-axes length. Thus, the aggregate–matrix structure is generated in two steps:

(i) *Particle generation*, i.e., determination of size and shape of all aggregate particles in order to match the precise size distribution and aggregate content. Hence, the lengths of the largest middle axes are randomly selected within the bounds of two adjacent sieve sizes, and the smallest axes are directly calculated according to the specified roundness of the particle. The third axis is an intermediary value, randomly selected according to calculated bounds, which ensure that the particle is retained in the lower sieve;

(ii) *Particle allocation*, i.e., the placement of the particles in the 3-D Euclidian space. In this case, the centre point coordinates and axis directions are determined particle by particle starting with the largest ones. Initially, centre point coordinates and axes directions are randomly determined. Thus, if the particle is completely inside the specimen and does not overlap previously placed ones, the position is granted. Otherwise, stochastic–heuristic algorithm is employed to perform successive shifts and rotations in order to move the particle into the specimen boundary or remove overlapping of particles.

Note that the algorithm performs some local heuristic search in the neighbourhood of the initial random position, using rotation and translation moves. To attain more uniform size distribution, the shifts (translation moves) are performed in stepwise manner along heuristically determined directions, with step values proportional to the ellipsoid axes and step sizes controlled according to the aggregate scattering (low or high aggregate content). Rotations are simulated by random changes in the Eulerian angles.

The investigation of intersection of ellipsoids is a sufficiently hard problem to prevent a closed analytical solution. A numerical solution employing the Gröbner basis method and solution of Sturm sequences through computer algebra was devised for this case.

In the real process of concrete placing and compacting, the smaller particles are somehow adjusted by the settlement of the larger particles. The proposed mechanism allocates initially the large particles and simulate smaller particles, hitting others and bouncing back until they have reached their final position. This yields a more realistic structure than a purely random procedure. In addition, the shifts allow the allocation of the ellipsoid centres to any position of the 3-D space instead of to a limited number of planes.

3. Structural idealisation and analysis

During the last 30 years, the use of discrete models to describe the nonlinear behaviour of materials such as rock or concrete has gained growing popularity [5,6]. Each of such discrete models presents a set of different assumptions with regard to material idealisation, structural idealization, mechanical properties and material behaviour of discrete elements (fracture law). In addition, these models may differ also in the consideration of the material behaviour (pure brittle or more ductile) as well as in the consideration of the loading condition (tension or compression). Consequently, all of these models have been reported fairly successful in their specific purposes, but hardly efficient in describing the material behaviour in situations other than the ones on which they have been tailored. In the particular case of cementitious composites, this suggests that general-purpose tools may require certain level of flexibility to accommodate the effects caused by differences in the material compositions.

The model developed in this study combines many of the successful features of existing models and some supplementary new features. In addition, the simulation software developed in this study allows the selection of different softening functions, mechanical properties and probabilistic scattering for each material independently. It also allows a selection among four different framework-type elements: planar truss (4 *df*), planar frame (6 *df*), space truss (6 *df*) and space frame (12 *df*) elements.

The meshes are initially generated as perfect lattices. However, small nodal perturbations may be imposed to produce irregular meshes. The initially 2-D (square) grid consists of 4 nodes interconnected by four lateral elements and two diagonals, while the 3-D (cubic) grid consists of 8 nodes interconnected by 12 edge elements, 12 diagonals on faces and 4 internal diagonals.

The cross-sectional areas of the different classes of elements (edge, diagonals, etc.) are automatically set in such a way that the stiffness of the mesh matches the stiffness of the continuum (assuming the same elastic modulus E for all mesh elements). However, the implemented software allows for manually assigning different values for each class of elements.

The material types for the line elements are assigned by projecting the lattice onto the aggregate–matrix structure (Fig. 3) and detecting whether both element nodes lie inside of the same aggregate (aggregate material) or both element nodes lie in the matrix and the element does not intersect any aggregate (matrix material). Otherwise, the element is considered as a bond interface between the two other materials. Hence, in the case of consideration of perfect bonding, the material stiffness of each bond interface element is assigned proportionally to the amount of each of the two materials in the element. In case of consideration of weak bonding, the interface element is considered as a third and independent material.

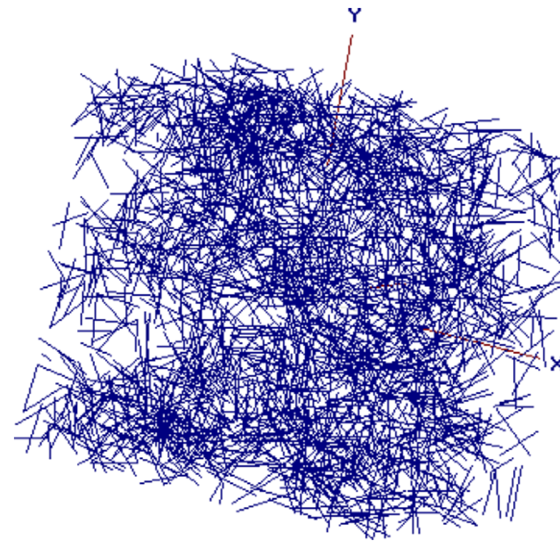

Fig. 4. Arrangement of fibres in 3-D discrete specimens.

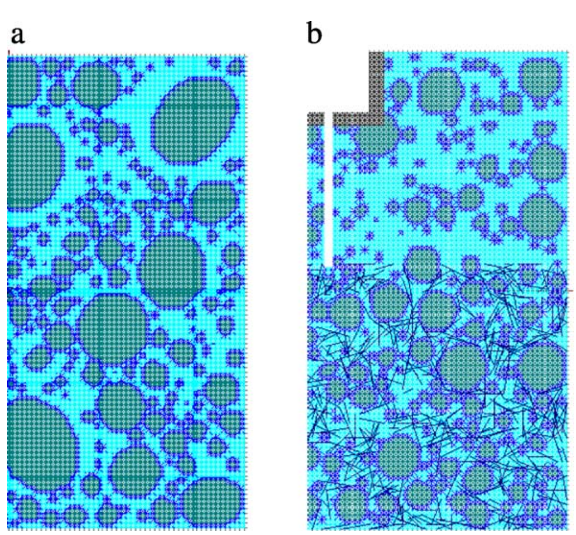

Fig. 3. Details from 2-D discrete specimens: (a) structure matrix–interface–aggregate for tension/compression simulations; (b) FRC structure for wedge-splitting simulations.

The most common approach that has been employed by various researchers to simulate the material behaviour and overall fracture process is the employment of a failure criterion for determining the collapse of discrete elements, after which the elements are removed. Thus, after an initial linear response, a nonlinear behaviour is obtained because of the successive failure of the elastic–brittle discrete elements. This approach seems apparently simple but also dependent on the size of the discrete elements. In this work an alternative approach, which includes a tensile softening branch in the material law of the discrete element, was implemented, assigning different softening laws in tension and compression for the different materials. The tensile softening functions are described on the basis of stress crack-opening laws. In order to adjust the elastic moduli of the softened elements at each step of the analysis, a number of procedures have been implemented for the different structural element types. The stress analysis is carried out in incrementally stepwise manner under displacement control using a direct solver.

The effect of fibre reinforcement was also modelled by introducing additional elements connecting distant mesh nodes in the matrix media after the generation of the matrix–aggregate structure. Since the allocation of fibres is associated with the mesh structure, the fibres are independently placed in 2-D and 3-D concrete structures by different algorithms. Fig. 3b shows details of a half specimen from 2-D wedge-splitting simulation. Note that in such a case, for computational convenience the fibres were placed only in the lower half of the specimen. In Fig. 4, the aggregate structure and mesh elements were made invisible to show the arrangement of the fibres in a 3-D simulation. For fibre-reinforced concrete, a softening function was derived on the basis of a bond–slip relation in order to describe the behaviour of the elements representing fibres.

4. Numerical simulations and discussion

Extensive parametrical analysis over a large number of simulations was carried out to investigate the effects of different model assumptions as well as the influence of different properties of the constitutive materials and different compositions on the mechanism of failure and on the properties of the composite material. Only a few selected results and brief descriptions of the simulations are to be presented here, since a detailed discussion on the results of the parametrical analysis is far beyond the scope of a single publication. In the initial set of the numerical simulations, the most common assumptions used by most models were investigated under different load conditions. This first set was particularly useful in a development stage to define or develop the features of the current model. The second set of simulations demonstrates some features and applications of the model presented here.

4.1. Model development stage

The following conventional assumptions for mesolevel model implementations, which have been proposed in the literature, were investigated at this stage:

- Geometrical properties of mesh elements are determined by setting the global stiffness of the mesh equal to the stiffness of the continuum, assuming mesh of homogeneous material and all elements with the same linear stiffness.
- The discrete concrete composition consists of elements of three different types of materials, namely, mortar elements, aggregate elements and the interfacial transition zone (ITZ) elements.
- Only coarse aggregate particles are generated and the surrounding matrix media (mortar) are considered to be homogeneous materials.
- ITZ is also considered as a homogeneous material, with mechanical properties assigned to considerably lower values than those of mortar.
- Values equivalent to those of mortar and aggregate testing specimens are assigned to the properties of the respective material elements.
- Overall softening effect is usually obtained by the removal of elements that fail under a fracture law.
- The concrete (matrix–aggregate) structure and mesh topology are generated on the 2-D space and scaled up by a thickness *t* of the fictitious slice (due to the physical and implementation complexity, models rarely generate concrete structure and mesh topology in the 3-D space, considering the entire depth of the specimen at once in the structural analysis).

Under certain specified conditions, the above-mentioned assumptions seem apparently sufficient for capturing the overall features of the failure behaviour and crack pattern observed in experimental studies. However, inconsistencies appear as soon as different material compositions and load conditions are investigated.

The development of the cracking surface along the aggregate–matrix interface led most numerical models to assign considerably lower values to ITZ element stiffness and strength lower than that of the adjacent mortar. However, simulations results of direct tensile tests of specimens with different aggregate content, assuming low strength values for ITZ elements, showed a considerable loss of overall strength, directly proportional to increasing of aggregate contents, which disagree with experimental results. The cracking surface quickly developed around aggregates and the connecting surface of mortar became the resistant material. Hence, increasing of aggregate content results in reduction of the resistant mortar surface and consequent loss of strength. On the other hand, when the strength of ITZ elements was assumed equivalent to that of mortar elements, there was little increase in global. The cracking remained developing as before, along interfacial zones, although eventually the crack path changed. In practice, there are some alterations in material microstructure and, consequently, in mechanical properties due to differences in the admixture, yet the growth of the crack surface imposed by the rise of the aggregate content seems to offsetting most of the loss in strength. The cracking pattern seems rather a result of localised stresses in the ITZ, which as observed in experimental studies [7] arise in particular from the difference of deformability between mortar and aggregates.

Stress–strain curves of four independent simulations of direct tension are presented in Fig. 5. In such simulations, the aggregate shape and stiffness were varied and an exponential tensile softening function was used to bring about the fracture process. Strength values for ITZ elements slightly lower than those assumed for the mortar were sufficient to enforce the same crack path as in the case of assuming weak elements, with the effect of crack bridging and development of the crack surface along the weaker ITZs in agreement with experimental results. The effect of aggregate shape/size is also captured in terms of ductility of stress–strain curves. The use of aggregates of ellipsoidal shape with the shortest-to-longest axis ratio (r) of 0.75 usually produced an increase of fracture toughness when compared to the effect of nearly spherical aggregates. This may be explained by the increase in crack surface, depending on the orientation of the aggregates along the crack path. The use of softer aggregates resulted in natural loss of global stiffness yet little increase in the overall strength, which may be attributed to the reduction of stress concentration along matrix–aggregate interfaces.

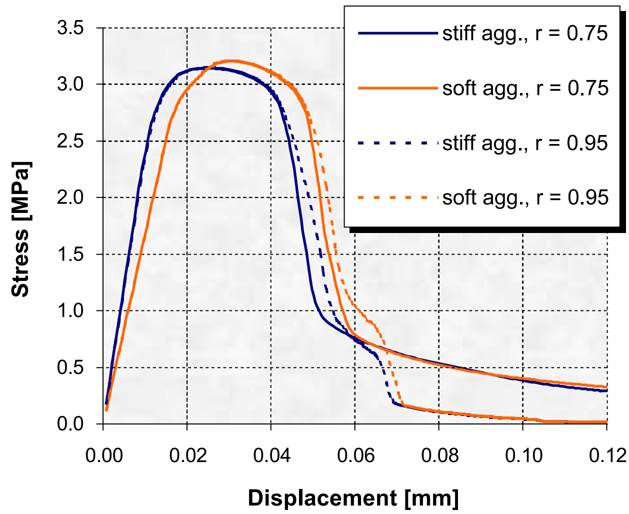

Fig. 5. Numerical simulations of concrete specimens in tension, using conventional model assumptions.

In simulations of compressive tests, since the fracture process is considerably more complex than in tension, implementation problems escalate and the above-mentioned assumptions are insufficient to cast the diffuse cracking pattern. The observed characteristic failure in compression may be described as a single diagonal shear crack band cutting through the specimen, which does not correspond to experimental results. The assumption of relatively weak interface results in loss of global stiffness, with the overall compressive strength considerably underestimated compared to the estimated tensile strength and stress–strain curves showing a rather brittle failure. The application of a tensile softening function to decay the element stiffness proved insufficient to produce overall failure. Alternative approaches, which physically remove the elements that fail in tension/compression, eventually enforce the removal of neighbouring elements to prevent the structure turning into a "mechanism," i.e., prevent unrestrained motions of neighbouring elements. Neighbouring elements (directly or indirectly connected to the collapsed member) may have to be removed regardless of their state of stresses; thereafter, stresses are redistributed among the remaining mesh elements. Such numerical manoeuvring may result in removal of aggregate as well as mortar elements, and if a crack starts to run into an aggregate, a good part or even the entire aggregate may be gradually removed to allow the crack to run through. This results in artificial changes in the crack path and, depending on the aggregate content, in considerable loss of global stiffness.

Note in the first of the previously mentioned assumptions that maintaining all elements with the same stiffness automatically defines the value of Poisson's ratio (v) by the geometry of the mesh; for example, for a square-grid mesh this value is 0.33. Bear in mind also failure process in simulations with external tensile loading is primarily due to successive collapse of mesh elements (in tension) along the load direction, while failure in simulations with compressive loading is caused primarily by the collapse of elements (in tension) oriented across the loading direction. Hence, considering that the fracture process is nonlinear, simulated in stepwise manner by discrete cracking, it is unlikely that there exists an effective way of scaling the stress–strain diagrams in order to take into account the values of v for concrete admixtures.

Numerical simulations of mortar specimens were performed to investigate the assumption of nearly homogeneous material. Initially, no aggregate structure was generated and a standard deviation of 5% in values of element properties was assumed. The obtained stress–strain curve (Fig. 6) does not vaguely resemble experimental curves of direct tensile tests. The lack of a driving force for the crack resulted in development of cracking surface concurrently from both sides. The material showed a strain hardening of up to 50% of the yielding stress, depending on the Poisson's ratio of the structure. In the simulations shown in Fig. 6, different stiffness values were assigned to diagonal and edge elements of the mesh to yield a mesh with $v = 0.2$. The overall tensile strength was about 20% higher than the strength of the individual elements, compared to about 50% higher for mesh with $v = 0.33$. On the other hand, the compressive strength seemed highly underestimated when compared with the tensile strength. The crack developed diagonally, straight from one corner to the other. Similar crack patterns were observed in previous attempts to model concrete in compression by other researchers [8]. In particular cases of concrete under compressive loading a shear failure may occur; for most cases of practice the failure is caused by tensile stresses transversal to loading resulting in concurrent longitudinal cracks. In practice, it seems that such shear stresses are partially resisted and redistributed by the frictional forces in the composite granular material.

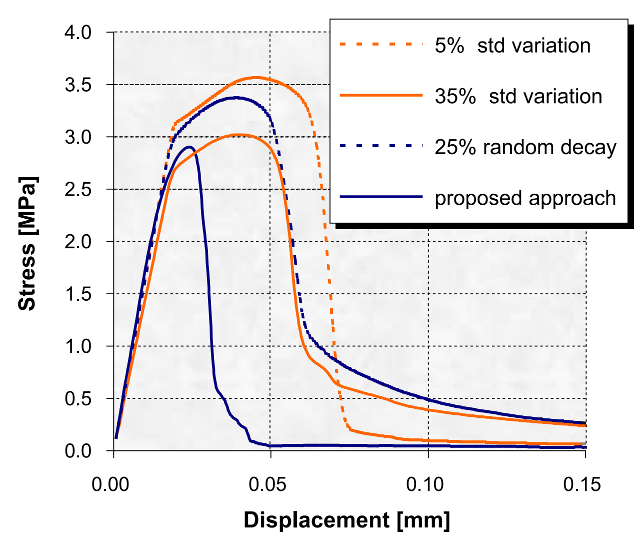

Fig. 6. Comparison of different approaches to simulate inhomogeneities in mortar specimens.

As described in the literature and mentioned above, mesolevel models only generate coarse aggregates, which usually represent less than 40% of the volume. Hence, the surrounding matrix (cement paste, voids and small aggregates), which is considered homogeneous, may be over 60% of the volume. Therefore, the assumption of mortar as nearly homogeneous material may be directly responsible or contributes largely to inconsistencies in the results. Inhomogeneities have been introduced in certain models either by a standard variation in the strength properties or by a randomly distributed decay in a percentage of elements. The effects of both approaches are also shown in Fig. 6. At high values of standard deviation (0.35) the shape of the curve only slightly improves but the overall tensile strength is still very high. The random decay seems to produce a better effect but is still insufficient. Both approaches are merely based on distribution of chaos at random, which has little chance of using problem-specific knowledge or bringing any enlightenment to the problem.

4.2. Model settlement stage

Translating experimental observations about weak properties of the ITZ into considerably low tensile strength seemed not to be an adequate approach for robust models. Alternative ways to introduce weakness in terms of degree of inhomogeneity of interface and mortar elements, which take into consideration the aggregate size distribution and other admixture information, are required.

In this stage, a number of the alternative approaches to correct possible flaws of mesolevel models were attempted and the implementations that showed best performance were put together to produce the final state of the model.

The properties of mortar elements were generated a priori over the entire mesh using a proposed approach in which a media of small aggregate particles is generated. The particles in consideration here are only those that are equal or larger than the mesh size, but are not to be considered in the fictitious concrete structure. These particles are used to identify some elements of the matrix whose material properties are equivalent to aggregate. Note that no interface elements were considered in this media of small aggregates. The properties of the remaining matrix elements are roughly estimated with basis on the aggregate properties considering (1) a decay in the properties somehow proportional to the fractions of different aggregate sizes in a Fuller distribution, which constitute the volume of the mortar, taking into account the grid size of the mesh and (2) the expected volume of the porous media. Standard deviations of a maximum 5% value were applied to the properties of the elements. This technique obviously introduces overheads in terms of computational effort, but it seems to pay off in performance. The resulting curve seems to be considerably improved (Fig. 6).

The concrete structure was generated thereafter and superposed over the existent mesh of mortar elements in order to determine the aggregate and ITZ elements, i.e., elements that lie partially inside of the aggregate. Hence, if mortar stiffness is assigned to ITZ elements, the loss of stiffness is proportional to the total aggregate surface. Although this loss may not be very substantial, two approaches were alternatively employed to circumvent this problem. The first approach calculates an equivalent modulus of elasticity proportional to the amount of both materials in the element. The second and perhaps more suitable approach scales up the stiffness of the aggregate by a factor proportional to the volume that is lost in the consideration of ITZ elements. For the aggregate elements the properties are completely reassigned, but for the ITZ elements only a small (0.10–020) reduction factor is randomly applied to the strength values. In the proposed model, failure was simulated by assigning an insignificant value to the member stiffness and, therefore, no member is physically removed. It was assumed that in a locally closed strut-tie system, the "failure" of tensile ties artificially increases the stresses in the compressive struts resulting in plastic deformation and failure of the compressive struts. Therefore, a softening function was introduced to account for the effect of the plastic deformation and eventual failure. Such set of implementations not only improved the curves but the crack patterns. In the simulations of compressive tests the crack pattern presented development of concurrent cracking surfaces, which did not happen before.

Simulations of direct tensile, uniaxial compression and wedge-splitting tests of FRC specimens were also carried out, but only after the adjustments on the settlement stage. For the 2-D analyses, an effective length of the fibre was assumed considering only the projection of the 3-D fibre on the plane of the 2-D slice cutout. In the results, the maximum load is only slightly influenced by the fibres, whereas the postpeak strength increases significantly with the fibre content, yielding more ductile fracture behaviour (Fig. 7). The crack pattern is more diffuse for the steel-fibre-reinforced concrete when compared to the plain concrete. The simulation results obtained for steel-fibre-reinforced concrete are in agreement with experimental observations. However, the 2-D model produces fairly rough curves and is limited to low-aggregate-content specimens or to the consideration of only large coarse particles. The increase of aggregate or fibre contents produces jamming of fibres in localised areas, resulting in temporarily increases in strength and, consequently, relatively sharp peaks on the curve. Such effect may be at certain extent observed in experimental testing, but using much higher aggregate and fibre contents than the ones employed in these simulations.

The curves and cracking pattern presented were obtained from 2-D analyses, because in this case the discrepancies are better displayed. The 2-D approach is commonly used not due to better performance, but due to difficulties in obtaining the 3-D concrete structure. Since the proposed model is based on a 3-D concrete structure, comparisons between 2-D and 3-D analyses could be performed. A specimen was

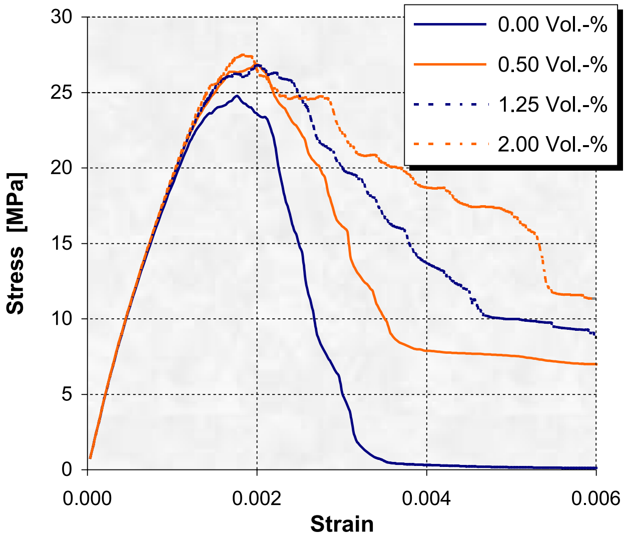

Fig. 7. Stress–strain curves of simulations of FRC in compression with various fibre contents.

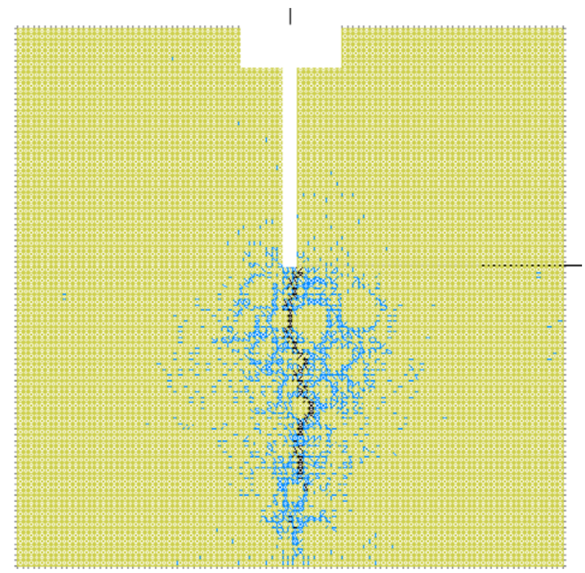

Fig. 9. Specimen of wedge-splitting simulation showing collapsed and softened members.

cut in many subsequent slices along the two axis directions perpendicular to the loading direction. The concrete structure was examined independently in the two directions. On average, the aggregate content of the slices is close to the content of the specimen and when the volume is integrated over a large number of slices it approaches the value specified for the aggregate volume. However, the aggregate content of individual slices may vary considerably from one to another. Consequently, the curves from assorted slices may be also quite different. In direct tensile tests, most cracking surfaces developed in the middle third part of the specimen and were roughly horizontal. However, in a number of slices, the cracking surface developed concurrently from two opposite sides of the specimen, thus, clearly showing that even considering only slices in a single direction, the cracking surfaces in the simulations were not the same. In fact, when the cracking surfaces of all slices in the two directions are plotted together in the 3-D space, they form a diffuse band instead of cracking surface. Therefore, the curves obtained in 3-D analyses have to be compared with the averaged curve of the slices of the same specimen. The averaged curve is more brittle and tends to overestimate the strength of the specimen as compared to the 3-D curve. The 3-D curves are less sensitive to variations of aggregate content when the interface is considered very weak, which suggests different assumptions from 2-D material properties. In FRC simulations, the 3-D curves are gentler than 2-D curves and considerably less sensitive to variations in fibre and aggregate contents.

Fig. 8 shows examples of cracking surfaces obtained in selected simulations of direct tension, uniaxial compression and wedge-splitting tests. The element displacements were scaled up to clearly present the crack pattern. The cracking patterns of simulations perfectly correspond to cracking surfaces obtained in experimental tests. In the wedge-splitting simulation of Fig. 8c, fibre reinforcement was used, resulting in change in the cracking path with slight increase in strength and considerable increase in ductility, as has also been observed in experimental tests. Fig. 9 presents the comparative cracking path in the case that fibres were not used. The dark lines show the members that have collapsed, while the intermediary colour shows the members that have entered into softening process due to the rising of localised stresses. The collapsed members show that in this case the crack runs straight below the notch, along the aggregate

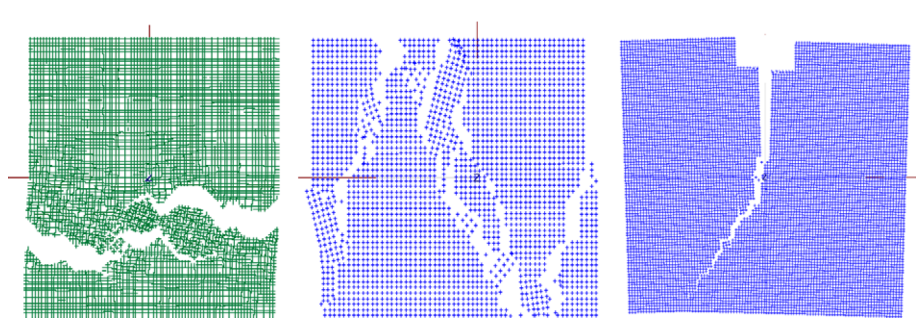

Fig. 8. Cracking pattern in simulations of direct tension (left), compression (middle) and wedge-splitting (right) tests.

interfaces. In the simulation, the stress distributions under the notch as well as stress concentrations along the aggregate interfaces were in perfect agreement with experimental observation.

Note that for the results presented here only 2-D and 3-D truss member types were employed.

5. Conclusions

Mesolevel models are prospective tools to describe both qualitative and quantitative effects of independent mechanical properties of different material components into the global mechanical properties of the composite material. Experimental studies can only statistically estimate such effects through analyses of samples, since two or more specimens with identical structure cannot repeat in experimental tests. In addition, in experimental tests it is hardly possible to investigate the influence of changes in properties of independent components, since changes in one component result usually in adjustment of other components and simultaneous changes in the micro- and mesoscopic structure.

Most mesolevel concrete models have been developed for simulations under tension. This is because the failure of concrete under tension is much more clear and easier to implement than under compression. However, model idealisations and assumptions, which are valid only for a particular loading situation, are mere artificial manoeuvres to mimic understood and well-defined features. They are not only inept to describe the real material behaviour but also unlikely to produce enlightenment and practical applications.

In simulations under compression, faced with the complexity of the failure mechanism, thorough investigations are yet required before sound conclusions may be drawn. However, comparisons between simulations of the same specimen under different loading conditions proved to be particularly useful for detecting inconsistencies in models and distinguishing assumptions that mimic the real-material behaviour from those that are merely numerical manoeuvres. Substantial effort should be introduced to enhance the performance of existing models under compression since there lie most application for concrete.

Although 3-D idealisations and analyses require more sophisticated setting and higher computational effort, they are clearly more accurate and naturally suitable for practical applications. The 2-D analyses suffer from a number of limitations and in general escalate the problems. On the other hand, they are more efficient to spot out the inconsistencies, and therefore particularly useful for model development.

The refined generation mechanism of the proposed model makes it suitable for both 3-D and 2-D analyses, with the advantage of dealing with a unique mesoscopic concrete structure. The more realistic concrete structure has allowed substantial enhancement in simulations of concrete under compression and reflects better understanding of the material behaviour.

References

[1] H. Sadouki, F.H. Wittmann, Modelling of microcracking induced by drying and endogenous shrinkage in cement composites, M.W. 2000, International Conference on Advanced Materials, Their Processes and Applications, Munich, Germany, Sept. 25–28, Werkstoffwoche-Partnerschaft GbR, Frankfurt, Germany, 2000.

[2] J.G.M. vanMier, E. Schlangen, A. Vervuurt, Tensile cracking in concrete and sandstone: Part 2. Effect of boundary rotations, Mater. Constr. vol. 29, Pergamon Press Ltd., Exeter, UK, 1996, pp. 87–96.

[3] A. Vervuurt, Interface fracture in concrete, PhD thesis, TU Delft, 1997.

[4] T. Stankowski, Numerical simulation of progressive failure in particle composites, PhD thesis, University of Colorado at Boulder, 1990.

[5] N.J. Burt, J.W. Dougill, Progressive failure in a model heterogeneous medium, J. Eng. Mech. Div. (ASCE) 103 (1977) 365–376.

[6] J.G.M. van Mier, Fracture mechanics applications, HERON 40 (2) (1995) 147–162.

[7] H. Mihashi, T. Sasaki, M. Izumi, Failure process of concrete: crack initiation and propagation, in: K.J. Miller, R.F. Smith (Eds.), Proceedings of the 3rd International Conference on Mechanical Behaviour of Materials, UK, August, vol. 3, 1979, pp. 97–107.

[8] K. Moriizumi, N. Shirai, Fracture and softening analysis of concrete with particle model, in: H. Mihashi, K. Rokugo (Eds.), Proceedings of the 3rd International Conference on Fracture Mechanics of Concrete Structures, Japan, May, vol. 2, Aedificatio Publishers, Freidburg, Germany, 1998, pp. 931–938.